

Origin of the different photoactivity of N-doped anatase and rutile TiO₂

Cristiana Di Valentin,^{1,2,*} Gianfranco Pacchioni,¹ and Annabella Selloni²

¹*Dipartimento di Scienza dei Materiali, Università di Milano-Bicocca, Via R. Cozzi, 53 - 20125, Milano, Italy*

²*Department of Chemistry, Princeton University, Princeton New Jersey 08540, USA*

(Received 7 May 2004; published 30 August 2004)

We have investigated the origin of the experimentally observed change in photoactivity of anatase and rutile TiO₂ induced by substitutional N-doping using state-of-the-art density functional theory calculations. Our results show that in both polymorphs N $2p$ localized states just above the top of the O $2p$ valence are present. In anatase these states cause a redshift of the absorption band edge towards the visible region. In rutile, instead, this effect is offset by the concomitant N-induced contraction of the O $2p$ band, resulting in an overall increase of the optical transition energy. Experimental trends are well described by these results.

DOI: 10.1103/PhysRevB.70.085116

PACS number(s): 71.55.-i, 71.15.Mb, 71.20.Nr, 78.20.-e

Photochemistry is one of the most promising technological applications of TiO₂.¹⁻³ TiO₂ is biologically and chemically inert, stable to corrosion, non-toxic and relatively inexpensive. Among various semiconductors, TiO₂ has proven to be the most suitable for environmental applications and has been widely employed to promote photocatalytic degradation of harmful organic compounds.¹ The main drawback of TiO₂ for photocatalysis is that its band gap is rather large, 3.0–3.2 eV, and thus only a small portion of the solar spectrum is absorbed in the UV region ($\lambda < 380$ nm). Hence, a large effort has been made to prepare doped TiO₂ with the absorption edge shifted towards the visible light region, as this would result in a tremendous improvement of photocatalytic efficiency. Many attempts have been made in this direction and various transition metal (TM) doped TiO₂ systems which absorb in the visible region have been synthesized.⁴ Unfortunately, the photocatalytic activity and photostability of these systems are rather poor. Absorption in the visible region is not always accompanied by photocatalytic properties since the photoproduced electrons (e_{cb}^-) and holes (h_{vb}^+) may not be available for chemical reactivity.

Doping with nonmetal atoms seems to be more successful.⁵⁻⁸ In particular, the presence of substitutional N atoms in the TiO₂ matrix (mixed anatase-rutile films,^{5,9} anatase films,¹⁰ powders,^{5,11,12} or nanoparticles¹³) improves absorption in the visible region and leads to a corresponding photochemical activity. The origin of this phenomenon is controversial. Based on spin-restricted LDA calculations on anatase Asahi *et al.*⁵ proposed a narrowing of the TiO₂ band gap due to mixing of N with O $2p$ states in the valence band. By contrast, photoelectrochemical measurements⁹⁻¹² have been interpreted as due to the presence of localized N $2p$ states. The picture is even more confused for the rutile polymorph of TiO₂, for which Diwald *et al.*¹⁴ have measured a blueshift of the photochemical activity (O₂ photodesorption) using single crystals, while Morikawa *et al.*¹⁵ observed a redshift of the adsorption edge using powders. The redshift is the typical behavior in N-doped anatase and anatase-rutile mixed systems.

To obtain microscopic insight into the effect of N doping on the photochemical activity of rutile and anatase, we have carried out an accurate comparative analysis of the atomic

and electronic structures of N-doped TiO₂ rutile and anatase for various levels of N doping, using spin-polarized DFT calculations within the generalized gradient approximation (GGA). We show that even for relatively high N concentrations the impurity states are localized and lie slightly above the top of the O $2p$ valence band. The shift in optical absorption has a different sign in rutile and anatase because of the contraction of the O $2p$ band in rutile upon doping. The results provide a solid basis for the rationalization of recently observed redshifts (anatase) and blueshifts (rutile) in photoactivity as a consequence of N doping.

The computations have been done using the plane-wave-pseudopotential approach, together with the Perdew-Burke-Ernzerhof (PBE)¹⁶ exchange-correlation functional, and ultrasoft pseudopotentials¹⁷ (with kinetic energy cut-offs of 25 and 200 Ry for the smooth part of the electronic wave functions and augmented electron density, respectively). Two independent codes were employed: CP90, based on the Car-Parrinello (CP) approach,^{18,19} which is particularly efficient for structural optimizations but has k -point sampling restricted to Γ , and the PWSCF package,²⁰ which was used to perform calculations at a low-symmetry k point (hereafter denoted K_{LS}). We considered nearly cubic $2\sqrt{2} \times 2\sqrt{2} \times 1$ and $2 \times 2 \times 3$ supercells to model anatase and rutile, respectively. The optimized bulk lattice parameters are taken from previous calculations,²¹ in which the same approximations of this work were used. N doping was modeled by replacing 1, 2, or 3 oxygen atoms in the 96-atom anatase supercell and 1 or 2 oxygen atoms in the 72-atom rutile supercell. The resulting stoichiometry is TiO_{2-x}N_x with $0.031 < x < 0.094$ for anatase and $0.042 < x < 0.084$ for rutile, comparable to that used in the experiments. The procedure of including more N atoms in the same supercell is more accurate than using smaller supercells as it allows a direct comparison of the various levels of doping on the band structure of the material. Atomic relaxations were carried out until all components of the residual forces were less than 0.025 eV/Å. When examining the relative positions of valence and conduction band edges (E_v and E_c , respectively) and impurity states, the Ti $3s$ levels, which in pure and N-doped rutile and anatase are practically at the same energy, have been aligned to each other. Values computed at K_{LS} are discussed, although values at Γ are also reported in Table I.

TABLE I. Energy differences in eV according to Fig. 3, computed at K_{LS} (values in italic computed at Γ).

n^a	W	E_1	E_2		E_3		E_4
			α	β	α	β	
anatase							
0	4.5	2.61					
	<i>4.5</i>	<i>2.19</i>					
1	4.4		2.48	2.30	0.14	0.32	
	<i>4.5</i>		<i>2.05</i>	<i>1.90</i>	<i>0.16</i>	<i>0.27</i>	
2	4.4		2.49	2.33	0.15	0.31	
	<i>4.4</i>		<i>2.08</i>	<i>1.93</i>	<i>0.15</i>	<i>0.30</i>	
3	4.3		2.50	2.36	0.17	0.33	
	<i>4.4</i>		<i>2.10</i>	<i>1.94</i>	<i>0.16</i>	<i>0.31</i>	
rutile ^b							
0	5.3	2.13					
	<i>5.7</i>	<i>1.81</i>					
1	4.9		2.21	2.25	0.38	0.29	0.43
	<i>5.0</i>		<i>2.31</i>	<i>2.40</i>	<i>0.61</i>	<i>0.42</i>	<i>0.79</i>
2	4.8		2.19	2.26	0.51	0.33	0.52
	<i>4.9</i>		<i>2.30</i>	<i>2.46</i>	<i>0.69</i>	<i>0.38</i>	<i>0.85</i>

^aNumber of N atoms per unit cell.

^bFor rutile results refer to geometries optimized at K_{LS} .

Experimentally, anatase has a slightly larger band gap (E_1) than rutile, 3.2 (Ref. 22) versus 3.0 eV (Ref. 23). The difference is somewhat overestimated in the calculations: $E_1=2.61$ and 2.14 eV for anatase and rutile, respectively, at K_{LS} (2.19 and 1.81 eV, respectively, in Γ), see Table I. The band gaps are underestimated, as usual in DFT. The primary structural difference between the two phases is that anatase is 9% less dense than rutile, and has larger Ti-Ti distances, a more pronounced localization of the Ti 3d states and a narrower 3d band.^{24–26} This entails that a carrier (electron) generated in anatase by UV excitation is less mobile than in rutile. Also the O 2p-Ti 3d hybridization is different in the two structures (more covalent mixing in rutile), with anatase exhibiting a valence and a conduction band with more pronounced O 2p and Ti 3d characters, respectively.²⁴ In rutile the greater Pauli repulsion among the oxygen 2p electrons results in a larger O 2p bandwidth (denoted as W in the following). Experimentally, $W(O\ 2p)$ in rutile is 6 eV (Ref. 26) while it is 4.7 eV (Ref. 27) in anatase. Our calculated values, 5.3 and 4.5 eV, respectively, nicely reflect this important difference in the electronic structures (Table I).

Replacing an O with a N atom in anatase does not result in significant structural changes. The Ti-N bond length, 1.964 and 2.081 Å, are only slightly longer than the Ti-O ones, 1.942 and 2.002 Å [Fig. 1(a)]. Therefore, the electronic changes due to the structural modifications are minor. The inclusion of a N atom in the lattice results in a paramagnetic impurity and in a doublet ground state. The unpaired electron has a strong N 2p character, and is largely localized on the N atom, with small tails extending on the nearest O atoms [Fig. 2(a)]. Considering the tendency of DFT calculations to produce delocalized spin states, this is a good evidence for the localized nature of the impurity state.

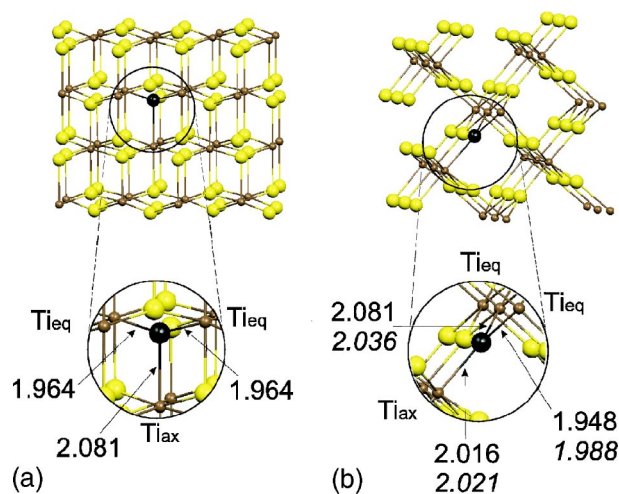


FIG. 1. N-doped TiO_2 (a) anatase (96-atom) and (b) rutile (72-atom) supercells. Bond lengths in Å (computed at Γ ; values in italic refer to K_{LS}). For comparison, the Ti-O bondlengths of undoped anatase (rutile) are 1.942 (1.956) and 2.002 (1.999) Å.

Analysis of the electronic energy levels shows that in N-doped anatase there is virtually no shift of the position of both top and bottom of the O 2p valence band, as well as of the conduction band, with respect to the undoped material (see Table I and Fig. 3). This is in contrast with the conclusions of Asahi *et al.*⁵ In addition to the singly highest occupied α_z state, nitrogen has four additional 2p electrons α_x and α_y and the corresponding β_x and β_y counterparts. In particular, the α_z state associated to the N dopant lies 0.14 eV above E_v (see E_3 in Fig. 3), while the empty β_z state lies about midway between the valence and the conduction bands. Thus, the N impurity can act as a deep electron trap in the material. Also the α_x , α_y , β_x , and β_y N 2p states lie slightly above the O 2p valence band (Table I). The energy difference between these localized states and the conduction band, E_2 in Fig. 3, is about 0.2 eV smaller than in pure anatase and the band gap transitions are reduced by the same amount (Table I). The presence of localized states above the valence band is consistent with the interpretation of recent photocatalytic experiments,^{9–12} and provides an explanation of the enhanced optical absorption in the visible region (in the range of 400–550 nm) observed for N-doped TiO_2 anatase. For simplicity, in the following we restrict the discus-

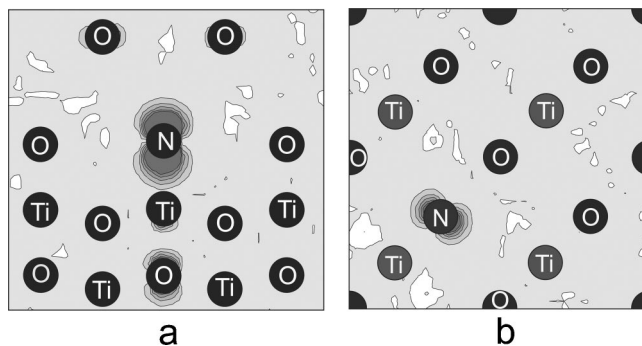


FIG. 2. Electron density corresponding to the highest singly occupied state in N-doped TiO_2 . (a) Anatase, (b) rutile.

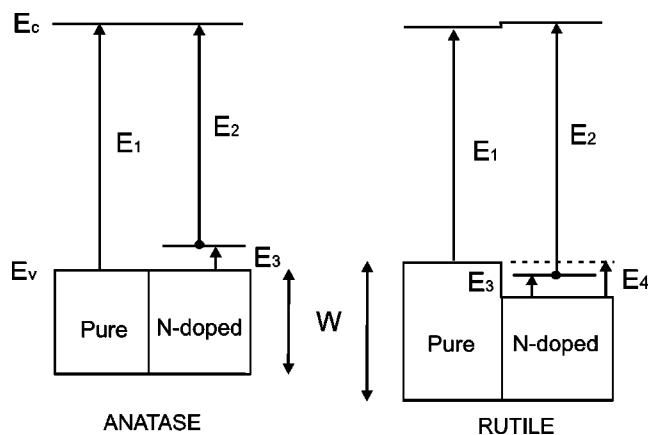


FIG. 3. Schematic representation of the band structure of pure and N-doped anatase and rutile. Energies are not in scale.

sion to the α set of states, since the same trends (even more pronounced) are observed for the β set, as reported in Table I.

Higher dopant concentrations have been simulated by replacing two and three oxygen atoms in the 96-atoms anatase supercell. The positions of the substitutional N atoms were chosen so as to maximize their mutual distance. Since every N atom introduces an unpaired electron, the total spin multiplicity is triplet (in the case of two N impurities), and quartet (for three N), assuming maximum multiplicity. Despite the relatively high doping, up to 5% with three N atoms, the structural modifications are small and similar to those observed for a single N impurity. The electronic structure is always characterized by the presence of a number of localized N $2p$ states just above E_v . The states maintain a rather well localized character, and the mixing with the O $2p$ levels is small. Of course, higher levels of N doping are expected to result in the formation of a continuum of states and in a consequent real shift of the top of the valence band. However, the experimental concentration of N atoms in the TiO_2 matrix is always very small, even below the minimum concentration considered here, $\text{TiO}_{1.969}\text{N}_{0.031}$ (notice that a much higher concentration, $\text{TiO}_{1.875}\text{N}_{0.125}$, was assumed in a previous theoretical study).⁵ At higher levels of doping, our results show a small shift of E_c towards higher energies (~ 0.05 eV in the case of three N atoms per supercell). This shift is overcompensated by the presence of N-derived states just above the valence band, so that the excitation energy E_2 from these states to the conduction band is reduced by ≈ 0.1 eV compared to pure anatase.

For the rutile TiO_2 polymorph, the structural variations following the replacement of one O atom with N in the 72-atom supercell appear to be more pronounced than for anatase. The equatorial $\text{Ti}_{\text{eq}}\text{-N}$ bonds (1.988 and 2.036 Å) are asymmetrically stretched with respect to the corresponding bonds in undoped rutile (1.956 Å), while the axial $\text{Ti}_{\text{ax}}\text{-N}$ bond is slightly stretched [2.021 vs 1.999 Å, see Fig. 1(b)]. As for anatase, the spin density is largely localized on the N atom [Fig. 2(b)]. The electronic structure shows both analogies and differences with respect to anatase. The main difference is a contraction of the valence band width, $W(\text{O } 2p)$. Since the position of the bottom of the band does

not change, this results in a lowering of E_v by 0.43 eV with respect to the undoped case, see E_4 in Fig. 3. The highest N induced level is 0.38 eV above E_v , hence the N $2p$ localized states are slightly lower in energy (0.05 eV) than E_v in pure rutile, see Fig. 3 and Table I. This shift of the occupied states is accompanied by a modest shift (0.03 eV) of E_c to higher energies. The consequence is that N doping in rutile is predicted to produce a small blueshift of 0.08 eV in the optical absorption and not a redshift, as observed for anatase. The replacement of a second oxygen by N in the 72-atom rutile supercell does not change these conclusions. The electronic and geometric structures are in line with those discussed for the single N impurity case. Therefore, a small blue-shift in the optical absorption energy is expected also for higher levels of N doping. This conclusion is entirely consistent with recent measurements of Diwald *et al.*¹⁴ on N-doped rutile TiO_2 single crystals.

The different behavior of rutile and anatase can be rationalized by considering the differences in the structure and electronic properties of these two polymorphs. Compared to anatase, rutile has a wider O $2p$ band, due to both its higher density, and its different structure. For instance, test calculations on a rutile supercell with the volume expanded by 9% yield an O $2p$ bandwidth 12% smaller with respect to the bandwidth for the regular supercell. In regular rutile, the removal of one electron from the volume of the cell, resulting from the replacement of one O with N, leads to a reduction of the Coulomb repulsion and a contraction of the band. This effect is found to be less pronounced in expanded rutile, where the repulsion is already significantly reduced. The same effect is also present in anatase, but it is in this case much weaker and practically irrelevant. Therefore in anatase the change in the absorption energy upon doping is determined by the occurrence of N-induced states above the top of the O $2p$ band, and the net effect is a reduction of the optical threshold energy.

One open question is the role of oxygen vacancies (V_{O}) in the visible light sensitivity and in the photocatalytic activity of both doped²⁸ and undoped²⁹ TiO_2 . Experimental estimates place the position of these states in rutile 0.75–1.18 eV below E_c (Ref. 30) (about 0.3 eV below E_c , in our calculations). Electrons trapped in these high-energy states can be easily excited into the conduction band, thus accounting for the blue coloring and the electrical conductivity of reduced titania crystals. For large deviations from stoichiometry the formation of a vacancy-related band below the conduction band may also enhance TiO_2 absorption in the near UV-visible regions. However, the simultaneous presence of N impurities and oxygen vacancies may lead to $V_{\text{O}} + \text{N} \rightarrow V_{\text{O}}^+ + \text{N}^-$ charge transfer states which can also contribute to the photocatalytic activity. Work is in progress to clarify this point.

In summary, because of different structures and densities, N-doping has opposite effects on the photoactivity of anatase and rutile TiO_2 , leading to a redshift and a blueshift, respectively, of the absorption band edge. In both cases the doping is accompanied by the appearance of well localized N $2p$ states above the O $2p$ valence band but in rutile the shift of the top of the valence band towards lower energies leads to an increase of the band gap transition.

*Electronic address: cristiana.divalentin@mater.unimib.it

- ¹M. Hoffmann, S. T. Martin, C. Wonyong, and D. W. Bahnemann, *Chem. Rev. (Washington, D.C.)* **95**, 69 (1995).
- ²A. L. Linsebigler, G. Lu, and J. T. Yates, Jr, *Chem. Rev. (Washington, D.C.)* **95**, 735 (1995).
- ³A. Hagfeldt and M. Grätzel, *Chem. Rev. (Washington, D.C.)* **95**, 49 (1995).
- ⁴W. Choi, A. Termin, and M. R. Hoffmann, *J. Phys. Chem.* **98**, 13669 (1994).
- ⁵R. Asahi, T. Morikawa, T. Ohwaki, K. Aoki, and Y. Taga, *Science* **293**, 269 (2001).
- ⁶J. Yu, J. Yu, W. Ho, Z. Jiang, and L. Zhang, *Chem. Mater.* **14**, 3808 (2002).
- ⁷T. Umebayashi, T. Yamaki, S. Yamamoto, A. Miyashita, S. Tanaka, T. Sumita, and K. Asai, *J. Appl. Phys.* **93**, 5156 (2003).
- ⁸S. Sakthivel and H. Kisch, *Angew. Chem., Int. Ed.* **42**, 4908 (2003).
- ⁹T. Lindgren, J. M. Mwabora, E. Avendaño, J. Jonsson, A. Hoel, C.-G. Granqvist, and S.-E. Lindquist, *J. Phys. Chem. B* **107**, 5709 (2003).
- ¹⁰H. Irie, S. Washizuka, N. Yoshino, and K. Hashimoto, *Chem. Commun. (Cambridge)* **11**, 1298 (2003).
- ¹¹S. Sakthivel and H. Kisch, *ChemPhysChem* **4**, 487 (2003).
- ¹²H. Irie, Y. Watanabe, and K. Hashimoto, *J. Phys. Chem.* **107**, 5483 (2003).
- ¹³C. Burda, Y. Lou, X. Chen, A. C. S. Samia, J. Stout, and J. L. Gole, *Nano Lett.* **3**, 1049 (2003).
- ¹⁴O. Diwald, L. Thompson, E. G. Goralski, S. D. Walck, and J. T. Yates, Jr, *J. Phys. Chem. B* **108**, 52 (2004).
- ¹⁵T. Morikawa, R. Asahi, T. Ohwaki, K. Aoki, and Y. Taga, *Jpn. J. Appl. Phys., Part 2* **40**, L561 (2001).
- ¹⁶J. P. Perdew, K. Burke, and M. Ernzerhof, *Phys. Rev. Lett.* **77**, 3865 (1996).
- ¹⁷D. Vanderbilt, *Phys. Rev. B* **41**, 7892 (1990).
- ¹⁸R. Car and M. Parinello, *Phys. Rev. Lett.* **55**, 2471 (1985).
- ¹⁹K. Laasonen, A. Pasquarello, R. Car, C. Lee, and D. Vanderbilt, *Phys. Rev. B* **47**, 10 142 (1993).
- ²⁰S. Baroni, A. Dal Corso, S. de Gironcoli, and P. Giannozzi, <http://www.pwscf.org>
- ²¹M. Lazzeri, A. Vittadini, and A. Selloni, *Phys. Rev. B* **63**, 155409 (2001).
- ²²H. Tang, H. Berger, P. E. Schmid, F. Lévy, and G. Burri, *Solid State Commun.* **23**, 161 (1977).
- ²³V. E. Henrich, and R. L. Kurtz, *Phys. Rev. B* **23**, 6280 (1981).
- ²⁴R. Asahi, Y. Taga, W. Mannstadt, and A. J. Freeman, *Phys. Rev. B* **61**, 7459 (2000).
- ²⁵J. Muscat, V. Swamy, and N. M. Harrison, *Phys. Rev. B* **65**, 224112 (2002).
- ²⁶J. C. Woicik, E. J. Nelson, L. Kronik, M. Jain, J. R. Chelikowsky, D. Heskett, L. E. Berman, and G. S. Herman, *Phys. Rev. Lett.* **89**, 077401 (2002).
- ²⁷R. Sanjinés, H. Tang, H. Berger, F. Gozzo, G. Margaritondo, and F. Lévy, *J. Appl. Phys.* **75**, 2945 (1994).
- ²⁸T. Ihara, M. Iyoshi, Y. Iiyama, O. Matsumoto, and S. Sugihara, *Appl. Catal., B* **42**, 403 (2003).
- ²⁹I. Justicia, P. Ordejón, G. Canto, J. L. Mozos, J. Fraxedas, G. A. Battiston, R. Gerbasi, and A. Figueras, *Adv. Mater. (Weinheim, Ger.)* **14**, 1399 (2002).
- ³⁰D. C. Cronemeyer, *Phys. Rev.* **113**, 1222 (1959).